J Mater Sci (2012) 47:272–281
DOI 10.1007/s10853-011-5795-y

In situ preparation, morphology and electrical properties of carbon nanofiber/polydimethylsiloxane nanocomposites

Nabarun Roy · Anil K. Bhowmick

Received: 24 April 2011 / Accepted: 12 July 2011 / Published online: 26 July 2011

Abstract For the first time, a series of carbon nanofiber (CNF)/polydimethylsiloxane(PDMS)-based nanocomposites was prepared using in situ polymerization technique by critical manipulation of factors, such as method of preparation and chemical modification of filler. Quantification of the degree of dispersion was done by introducing a dispersion degree parameter. Extent of dispersion was found to improve by amine modification of CNFs. Electrical conductivity was found to undergo profound increase when compared with that of the insulating base polymer. Amine-modified CNF-based nanocomposites showed percolation threshold at lower filler loading compared with unmodified CNF-based nanocomposites. These results of electrical properties measurements were correlated with the results of TEM analysis.

Introduction

Recent developments in material science involve a novel and attractive approach of incorporation of nanoparticles into polymers, since this facilitates the development of new materials by exploring synergistic effects [1, 2]. The intriguing feature of these advanced materials includes improved thermal, mechanical, electrical, and selective permeation properties [3–5]. Although traditional composites contain significant amount of filler, dramatic improvement in properties is observed for low loadings of various nanofillers [6–9]. These improvements in properties are achieved by exploiting several factors, such as degree of dispersion, interface chemistry, and nanoscale morphology.

Of the carbon-based fillers, carbon nanotubes and carbon nanofibers (CNFs) exhibit intrinsic mechanical and electrical properties [10, 11]. However, due to high specific surface area and energy, these nanofillers tend to aggregate, which makes it very difficult to disperse homogeneously in the host polymer matrix. Surface functionalization is one of the way-outs which significantly improves filler dispersion [12, 13]. Polydimethylsiloxane (PDMS), on the other hand, possesses several virtues such as low temperature flexibility, high thermal stability, biocompatibility, etc. However, its poor electrical properties limit its gamut of applications. Thus, the main aim of this study is to improve the electrical properties of these insulating elastomers. Nanocomposite preparation facilitates improvement in various properties, provided proper dispersion of the filler is achieved.

Extensive literature survey reveals that no work has been done till date on CNF/PDMS nanocomposites. The probable reason for this is the huge surface energy difference of PDMS and CNF. PDMS is a semiorganic polymer with very low surface energy ($\sim$19.6 mJ/m^2) [14], whereas CNF has an appreciably high surface energy of 145–165 mJ/m^2 [15]. This restricts homogeneous dispersion of nanofibers in the polymer matrix. Thus, preparation of CNF/PDMS nanocomposites is itself challenging and novel. Moreover, the method of in situ preparation of nanocomposite through anionic ring opening polymerization is completely new. In this article, it is shown for the first time how the in situ preparation of nanocomposite affects the extent of dispersion in comparison with the conventional ex situ prepared nanocomposites. Furthermore, the effect of filler functionalization on properties of

N. Roy · A. K. Bhowmick (✉)
Rubber Technology Centre, Indian Institute of Technology, Kharagpur 721302, India
e-mail: anilkb@rtc.iitkgp.ernet.in; director@iitp.ac.in

A. K. Bhowmick
Indian Institute of Technology, Patna 800013, India

nanocomposites is also discussed here. This is done by quantifying the extent of dispersion by introducing a dispersion parameter, $D_{0.1}$. The detailed image analysis of the TEM images and quantification of the dispersion degree is also noteworthy. These results have been correlated with the electrical properties of the nanocomposites. It is well established that the filler functionalization of CNFs results in decreased electrical conductivity of the nanocomposites in comparison with that of the nanocomposites prepared with unmodified CNF [10]. However, in this study we have observed increase in electrical conductivity upon filler functionalization. This unique observation has been correlated with the morphology of the nanocomposites.

Experimental

Materials

Octamethylcyclotetrasiloxane $[(CH_3)_2SiO]_4$ (D_4) purity >99% (GC), Platinum catalyst and hydride crosslinker polymethylhydrogenosiloxane $Me_3Si(OSiMe_2)_x(OSiMeH)_y OSiMe_3$, where x and y are 10, having hydride content of 4.3 mmol/g were supplied by Momentive Performance Materials, Bangalore, India.

CNFs and Tetraethoxysilane (TEOS) were obtained from Applied Sciences Inc., USA and Acros Organics, New Jersey, USA, respectively. Dibutyltin dilaurate (DBTDL) was procured from Aldrich Chemicals, Bangalore, India.

Hexamethylenediamine (HMDA) was procured from Merck, Merck Schuchardt OHG, Germany. Potassium hydroxide was purchased from Merck, Mumbai, India.

Synthesis of pristine PDMS and PDMS-based nanocomposites

Surface functionalization of CNFs

3 g of nanofibers was treated with excess of HMDA at 130 ± 10 °C in an oil bath for 24 h. The amine-modified nanofibers were then washed with alcohol to remove the excess amine, followed by washing with distilled water to remove the alcohol present. These were then dried in vacuum oven at 80 °C for 4 h. Amine modification of CNF was done following the procedure of George and Bhowmick [16].

In situ synthesis and curing of PDMS-based nanocomposites

Calculated amount of CNF was soaked in 15 g of D_4 overnight followed by ultra-sonication. To this, 0.08 g of finely grinded KOH was added and polymerization reaction was carried out at 140 °C under nitrogen atmosphere for 2 h. The reaction was terminated after 2 h, and the reaction mixture was left overnight. The resultant nanocomposite was dissolved in toluene and unreacted base was neutralized by H_3PO_4. To this solution, calculated amount of TEOS was added and stirred for 5 min. This was followed by the addition of DBTDL and the resultant mixture was stirred for another 1 min. The stirred solution was cast on a petri dish and left undisturbed overnight. Complete evaporation of solvent yielded cured sheet of ~5-mm thickness which was vacuum-dried at 80 °C.

Ex situ preparation of CNF/PDMS nanocomposites by solution casting

For ex situ prepared nanocomposites, polymerization and work up was carried out following exactly the same procedure as for in situ prepared nanocomposites. Once the polymer was synthesized, CNF-based nanocomposites were prepared by conventional solution casting technique. Curing was done in the same way as that for in situ prepared nanocomposites. The samples along with their compositions and designations are compiled in Table 1.

Instrumentation

The samples for TEM analysis were prepared by ultracryomicrotomy with a Leica Ultracut UCT (Leica Microsystems GmdH, Vienna, Austria). TEM was performed using JEOL 2100, Japan at an accelerating voltage of 200 kV.

AC conductivity and permittivity of the composites were measured using LCR meter (model 819, Goodwill Instek Co, Taiwan). The measurements were carried out in a frequency range of 10–10^6 Hz. The resistance, capacitance, and dissipation factor (tanδ) values were directly measured from the LCR meter. From the values of capacitance and dissipation factor, the dielectric constants of the samples are calculated through the capacitance by the fundamental equation:

$$\varepsilon' = \frac{C \times t}{0.0885 \times A} \quad (1)$$

where C is the capacitance of the sample in picofarads, t is thickness of the sample in cm, and A is the area of the sample in cm^2.

AC conductivity (σ_{AC}) is evaluated from the dielectric data in accordance with the relation (Eq. 2).

$$\sigma_{AC} = \omega \varepsilon_0 \varepsilon' \tan\delta \quad (2)$$

where $\omega = 2\pi f$ (f is frequency in Hz), ε_0 is the permittivity of the vacuum, ε' is the dielectric constant or relative permittivity, tanδ is dielectric loss tangent or dissipation factor.

Table 1 Composition of the samples along with their designation

Sample	D_4 used (g)	KOH (g)	Polymer obtained (g)	Amount of TEOS (g)	Amount of CNF (with respect to the polymer obtained) (phr)[a]
PD C0	15	0.08	13	0.5	–
PD C1	15	0.08	13	0.5	1
PD C2	15	0.08	13	0.5	2
PD C4	15	0.08	13	0.5	4
PD C6	15	0.08	13	0.5	6
PD C8	15	0.08	13	0.5	8
PD C10	15	0.08	13	0.5	10
PD C1A	15	0.08	13	0.5	1
PD C2A	15	0.08	13	0.5	2
PD C4A	15	0.08	13	0.5	4
PD C6A	15	0.08	13	0.5	6
PD C8A	15	0.08	13	0.5	8
PD C10A	15	0.08	13	0.5	10
PD C1E[b]	15	0.08	13	0.5	1
PD C2E[b]	15	0.08	13	0.5	2
PD C4E[b]	15	0.08	13	0.5	4
PD C6E[b]	15	0.08	13	0.5	6
PD C8E[b]	15	0.08	13	0.5	8
PD C10E[b]	15	0.08	13	0.5	10

PD: hydroxyl PDMS, C: carbon nanofiber, A: amine-modified carbon nanofiber-filled nanocomposites

[a] Parts per 100 g of rubber

[b] Samples prepared by ex situ method

Results and discussion

Properties of pristine PDMS

Synthesis of PDMS and curing reaction

Synthesis of hydroxyl PDMS has been carried out according to the reaction scheme shown in Fig. 1. Curing of the elastomer has been carried out using TEOS and DBTDL following the principle of hydrolysis and condensation.

Characterization of nanocomposites

TEM studies

TEM images of unmodified and amine-modified CNF-based nanocomposites at same filler loading (4 phr) prepared by in situ and ex situ techniques are shown in Fig. 2. Figure 2a–c shows the representative high resolution TEM images of ex situ prepared nanocomposite with unmodified CNF, in situ prepared nanocomposite with unmodified CNF, and in situ prepared nanocomposite with amine-modified CNF, respectively. Figure 2d–f is their respective low resolution images. The bright background in the transmission electron micrograph is the polymer matrix, while the dark bamboo-like structures with hollow cores show the nanofibers dispersed therein. The reaction temperature and the other conditions imposed on the nanofibers during the polymerization reaction leads to structural breakdown of the nanofibers. Additional anchorage is provided by the defect sites thus generated. Thus, it can be clearly understood that the natural tendency of the nanofibers to aggregate is disturbed by the polymer matrix and this is the consequence of improved interaction between the two heterogeneous phases. Dispersion state of the filler in the nanocomposites was analyzed and hence quantified using ImageJ software as a tool. This software provides provision for background correction in which a "sliding paraboloid" or a legacy "rolling ball" algorithm has been used for correction of uneven illuminated background. The image has been subjected to smoothening to remove undesired noise and is then converted to a threshold image or 8-bit binary image. Figure 3a shows the threshold TEM image of in situ prepared 4 phr unmodified CNF loaded PDMS nanocomposite. The distance in pixels is converted into distance in μm. This enables finding the spacing between various features and hence can be employed to analyze the state of dispersion of filler in the nanocomposites.

The next step of analysis deals with determining the distance between nanofibers. A straight line selection tool

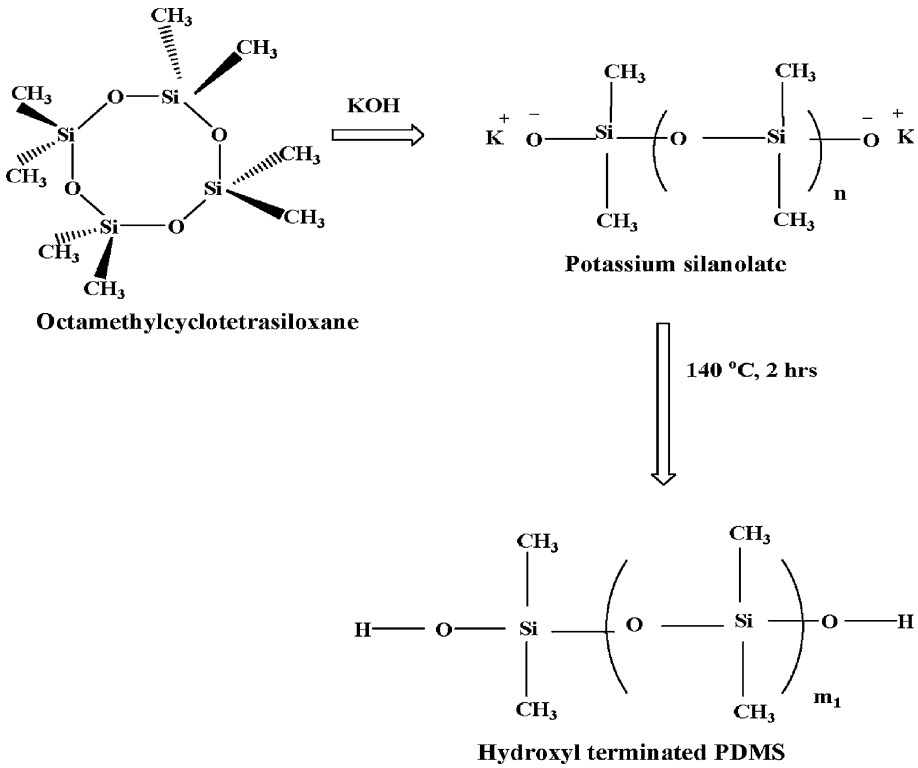

Fig. 1 Scheme of the polymerization reaction for hydroxyl PDMS

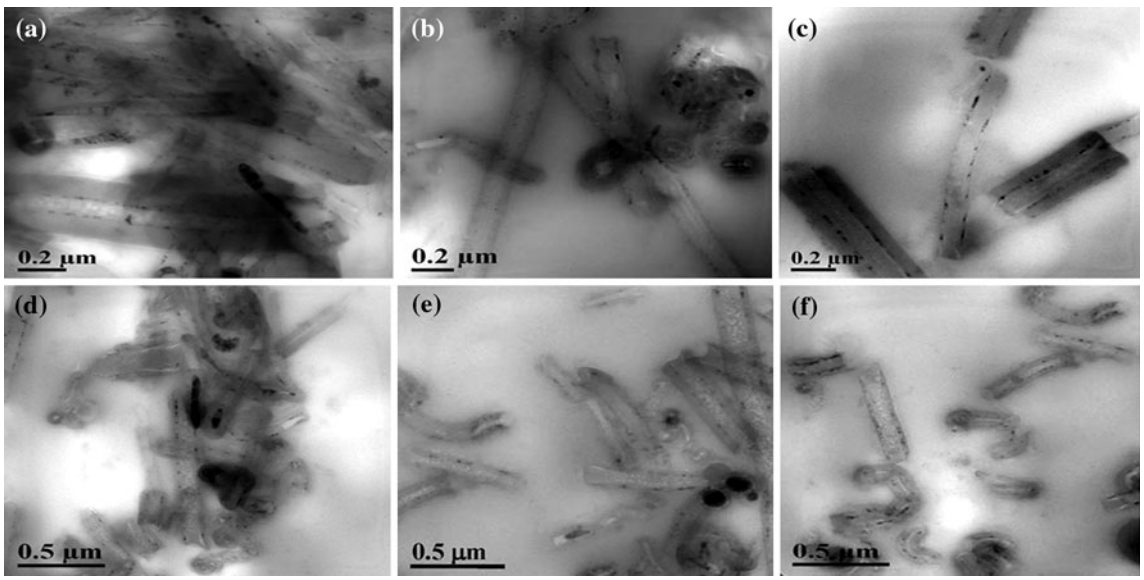

Fig. 2 TEM image of ex situ prepared unmodified CNF/PDMS nanocomposite(**a** at high resolution and **d** at low resolution), in situ prepared unmodified CNF/PDMS nanocomposite (**b** at high resolution and **e** at low resolution) and in situ prepared amine-modified CNF/PDMS nanocomposite (**c** at high resolution and **f** at low resolution) (filler loading 4 phr)

has been employed to specify the region scanned and a corresponding plot profile for the scanned area is obtained. Figure 3b shows a representative plot profile. In this plot, the distance in μm (*x*-axis) showing a zero gray value corresponds to the spacing between the nanofibers. This is due to the fact that the polymer matrix where nanofibers are dispersed has a zero gray value.

The threshold image can be viewed in three dimensions by plotting the interactive 3D surface plot shown in Fig. 3c. The *x* and *y* axes constitute the scanned region of the sample, but *z* axis specifies inverse of luminance of various parts of the scanned image. The portions having more gray value will have a greater height compared with those regions having lesser gray value. In other words, the

inverse of luminance of an image is a measure of the height for the plot. From the plot, it is quite clear that individual fibers are well separated by the matrix domain.

This methodology has been adopted and similar measurements have been done over the entire area of the TEM image, and a mean free path between the nanofibers has been estimated. This is followed by construction of a histogram of the spacing data which shows the free path distance distribution. Quantification of the extent of dispersion is achieved by the dispersion parameter, $D_{0.1}$ which is defined as the free path distance distribution. This lies in the range of $0.9\bar{x}$ to $1.1\bar{x}$, where $\bar{x}$ is the mean spacing between the nanofibers. $D_{0.1}$ is a dimensionless quantity and is related to the extent of dispersion. A higher $D_{0.1}$ value indicates more data close to the value of mean spacing, thereby suggesting better dispersion [17–19]. Free path distribution follows a lognormal distribution model [17] and $D_{0.1}$ is expressed as:

$$D_{0.1} = 1.1539 \times 10^{-2} + 7.5933 \times 10^{-2}(\bar{x}/s) + 6.6838 \times 10^{-4}(\bar{x}/s)^2 - 1.9169 \times 10^{-4}(\bar{x}/s)^3 + 3.9201 \times 10^{-6}(\bar{x}/s)^4 \quad (3)$$

where s is the standard deviation.

In order to estimate $D_{0.1}$, extensive measurements of the free path x_i (distance between the nanofibers) have been carried out. This is followed by calculation of $\bar{x}/s$ which is used in Eq. 3 to calculate $D_{0.1}$.

Figure 3d is the representative plot of frequency versus distance between the nanofibers for CNF/hydroxyl PDMS nanocomposite with 4 phr of filler loading. The unmodified CNFs are properly dispersed with very few lump formation or appearance of bundles. The free path distance is calculated, and the sampling number is $N = 260$. The histogram showing the free path distance distribution is plotted as shown in Fig. 3d. A lognormal dispersion model is impressed which is followed by the calculation of $D_{0.1}$ using Eq. 3. From the lognormal fit, the mean spacing and standard deviation are calculated to be $\bar{x} = 0.335\ \mu$m and $s = 0.109\ \mu$m, respectively. This results in $\bar{x}/s = 3.073$ and hence a $D_{0.1}$ value of 24.56%.

Mode of nanocomposite preparation has a profound effect upon the degree of dispersion. Fig. 4a, b shows, respectively, the 3D interactive images of ex situ prepared unmodified CNF/hydroxyl PDMS nanocomposite and in situ prepared amine-modified CNF/hydroxyl PDMS nanocomposites with

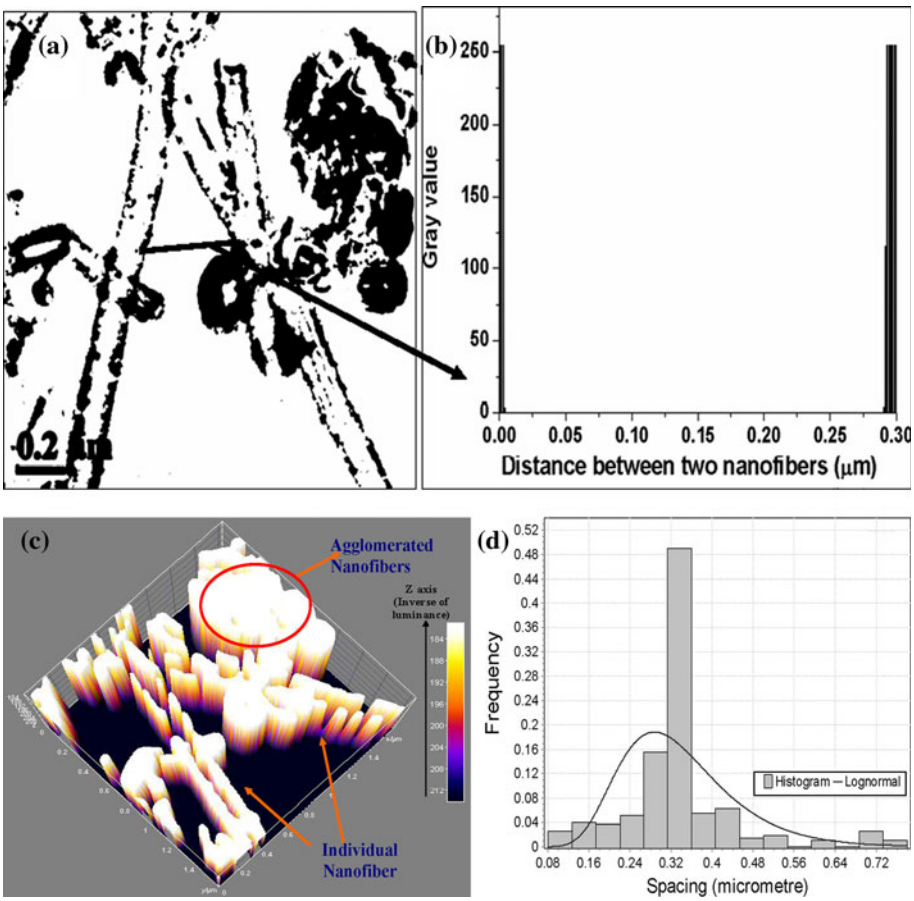

Fig. 3 **a** Threshold TEM image of in situ prepared unmodified CNF/hydroxyl PDMS nanocomposite. **b** Plot of gray value versus distance for the selected region in the threshold TEM image of the nanocomposite. **c** Representative 3D interactive plot for in situ prepared unmodified CNF/hydroxyl PDMS nanocomposite. **d** Plot of frequency versus distance between nanofibers in the in situ prepared nanocomposite

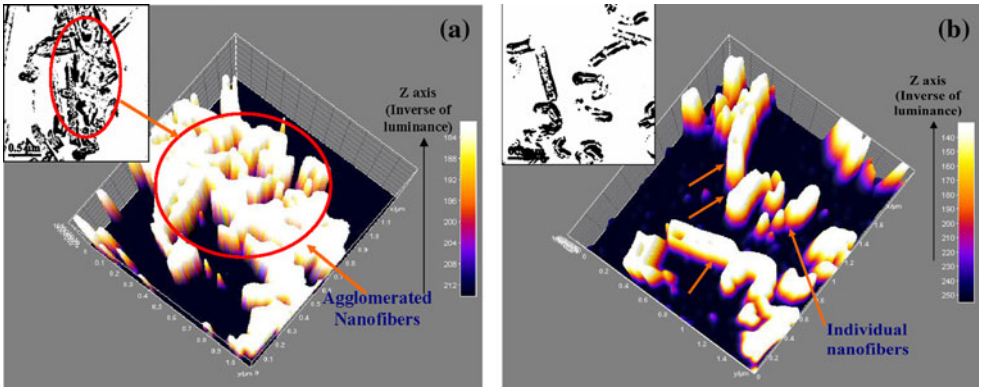

Fig. 4 **a** 3D interactive plot of ex situ prepared unmodified CNF/PDMS nanocomposite with the respective threshold TEM images in the *inset* (filler loading 4 phr). **b** 3D interactive plot of in situ prepared amine-modified CNF/PDMS nanocomposite with the respective threshold TEM images in the *inset* (filler loading 4 phr)

Table 2 Comparison of $D_{0.1}$ values for various samples

Sample	$\bar{x}/s$	$D_{0.1}$ (%)
PD C4	3.073	24.56
PD C4E	1.321	11.26
PD C4A	3.570	28.31

their respective threshold TEM images in the inset. The mean spacing between the nanofibers for ex situ nanocomposites is found to be $\bar{x} = 0.103\,\mu$m with a standard deviation $s = 0.078$ μm which results in $\bar{x}/s = 1.321$. This is evident from the TEM image in Fig. 2a, d. In this figure, carbon nanofibers are aggregated predominantly. Even $D_{0.1}$ is found to be 11.26% which is significantly lower than that of the in situ nanocomposite. This shows that a finer extent of dispersion is achieved by in situ method of nanocomposite preparation. This is probably by virtue of the method of nanocomposite preparation. In situ nanocomposite preparation facilitates polymer chain growth in the presence of the nanofibers. This provides enough scope for the nanofibers to be separated from each other aiding the process of deagglomeration.

Amine functionalization of CNF gives better degree of dispersion for the nanocomposites compared with those prepared using unmodified CNF. This is due to the fact that besides intrinsic van der Waals forces, amine functionalities on the fiber surface provide H-bonding interaction with the main polymer backbone thereby facilitating better dispersion as found in Fig. 2c, f. In this case, $\bar{x}$ and s are calculated to be 0.332 and 0.093 μm, respectively which gives $\bar{x}/s = 3.570$ and hence a $D_{0.1}$ value of 28.31%. Thus, filler dispersion is significantly bettered by functionalization of filler. These results are compiled in Table 2.

Electrical properties

Though the elastomeric PDMS matrix is insulating in nature, proper dispersion of the CNF in the matrix results in significant improvement in electrical conductivity. However, good dispersion is not just the only criteria for enhanced electrical properties. Figure 5a shows good dispersion of nanofibers. But the resultant hybrid material shows poor conductivity almost similar to that of the unfilled elastomer. On the other hand, Fig. 5b shows good dispersion and the nanocomposite shows good conductivity. The difference lies in the fact that in the latter one a conducting network is formed by the nanofibers which is absent in the former. Thus, formation of a conducting network facilitates improvement in electrical and dielectric properties of the nanocomposites.

Effect of method of nanocomposite preparation and filler functionalization on electrical conductivity

The ac conductivity was measured over a range of frequencies. The value of conductivity at the lowest measured frequency (10 Hz) has been considered as σ_{dc}, which is the dc electrical conductivity for the sake of study [20]. Conductivity increases with filler volume fraction (Fig. 6). In situ pristine CNF-based PDMS nanocomposites attain percolation threshold at 4 phr filler loading and show higher magnitude of dc electrical conductivity compared with those prepared by the ex situ method. Amine modified CNF-based nanocomposites show similar behavior; however, the percolation threshold is obtained at much lower loading i.e., 1 phr, as shown in Fig. 6. Conductivity for in situ amine-modified CNF-based system is even higher than those prepared with unmodified CNFs. σ_{dc} increases from 10^{-12} Scm^{-1} (base polymer) to 10^{-8} Scm^{-1} for just 1 phr of amine-modified CNF-filled nanocomposite, while it shows a minimal increase of 10^{-11} Scm^{-1} for ex situ prepared nanocomposites and 10^{-10} Scm^{-1} for in situ prepared nanocomposites with unmodified CNF for the same filler loading. However, the nanocomposites prepared with unmodified CNF shows conductivity of the order of 10^{-8} Scm^{-1} at 4 phr filler loading. Thus, it can be concluded that better dispersion in the case of amine-modified CNF-based nanocomposites facilitates formation of

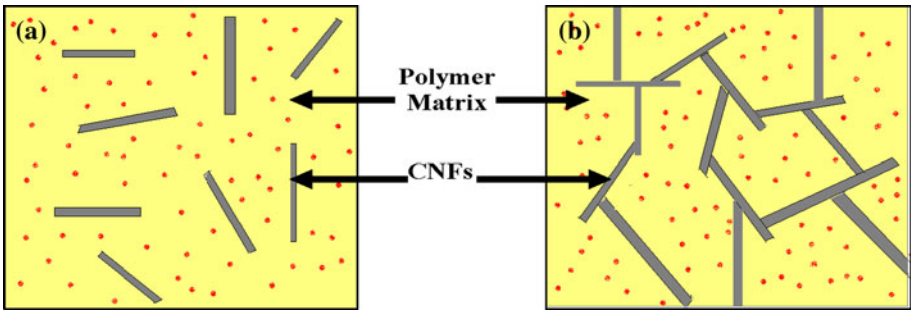

Fig. 5 Pictorial representation of nanocomposites **a** with good dispersion showing poor electrical conductivity **b** with good dispersion and enhanced electrical conductivity

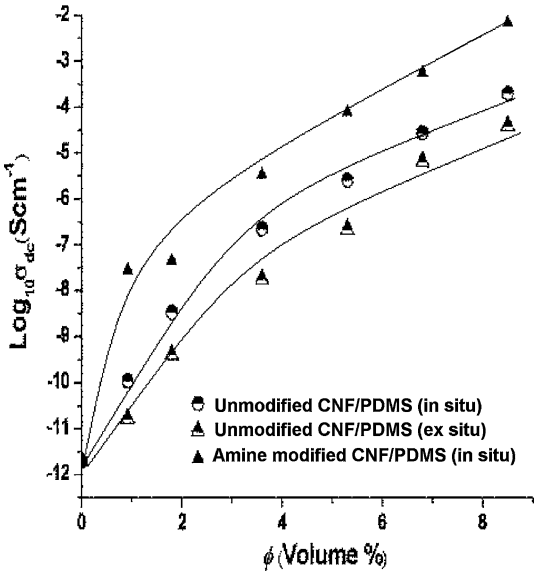

Fig. 6 Logarithm of dc electrical conductivity versus filler volume concentration

conducting network at 1 phr filler loading which results in this enhanced conductivity. On the other hand, unmodified CNF-based nanocomposites show the same network formation at 4 phr filler concentration. Thus, these nanocomposites attain percolation at a higher critical filler concentration compared with those prepared with modified ones.

Percolation theory [21, 22] has been employed to understand the σ_{dc} above ϕ_c by means of the following law:

$$\sigma_{dc} \propto (\phi - \phi_c)^t \tag{4}$$

t being a critical exponent dependent upon the dimensionality of the system.

Though theoretical calculations propose a value of 1.6 to 2 for t for fiber-like fillers [23–25], fitting of experimental data in Eq. 4 results in a t value of 4 which is higher than those reported in the case of fiber-like additives [26]. The value of t is obtained from the slope of the plot of Log σ_{dc} versus Log $(\phi - \phi_c)$ shown in Fig. 7a.

Thus, with a t value equal to 2, a higher value of ϕ_c results in the same value of dc conductivities. Hence, there may be some mechanism for charge transfer other than filler network formation which is prevalent at $\phi < \phi_c$. The tunneling conductivities [27] in MWCNT and CNF [21, 22] similar to carbon black [28–31] are observed at low filler concentration. In this case, charge carriers travel through the insulating gaps in the sample and hence are responsible for increased conductivities of the insulating material. The mechanism is depicted in Fig. 7b.

Approximately the mean average distance among the particles is proportional to $\phi^{-1/3}$ [32]. From the plot of Log σ_{dc} versus $\phi^{-1/3}$ shown in Fig. 7c, it is found that the data related to conductivities show a linear dependence. This deviation from the percolation model is due to tunneling conduction in the nanocomposites.

On the other hand, from Eq. 5, it is concluded that σ_{ac} is dependent on frequency. Conductivity almost remains constant with minute variations until a critical frequency F_c is attained. This is followed by a steady increase in conductivity with increase in frequency. Thus, σ_{ac} is related to frequency by the expression:

$$\sigma_{ac} \propto F^S \tag{5}$$

That particular value of frequency has been considered as F_c data at which 5% increase in conductivity is observed with respect to σ_{dc}. These values are employed to plot a graph displaying variation of Log F_c as a function of filler concentration shown in Fig. 8. It is found to show a linear dependence.

Though covalent functionalization improves nanofiber dispersion in solvents and polymers and hence improves mechanical and sometimes thermal properties of the nanocomposites, electrical properties suffer due to the disruption of the extended π conjugation through functionalization. This is because of the fact that these sites serve as the scatter site for electrons [33]. However, amine-modified CNF-based nanocomposites is found to be more conducting compared with the unmodified CNF based ones. Even functionalized CNFs show percolation threshold at lower filler loading. This increase in conductivity is probably due to better dispersion of the nanofibers in the

polymer matrix which facilitates the conducting network formation in the polymer matrix. Similar observations have been made with filler modification in some instances

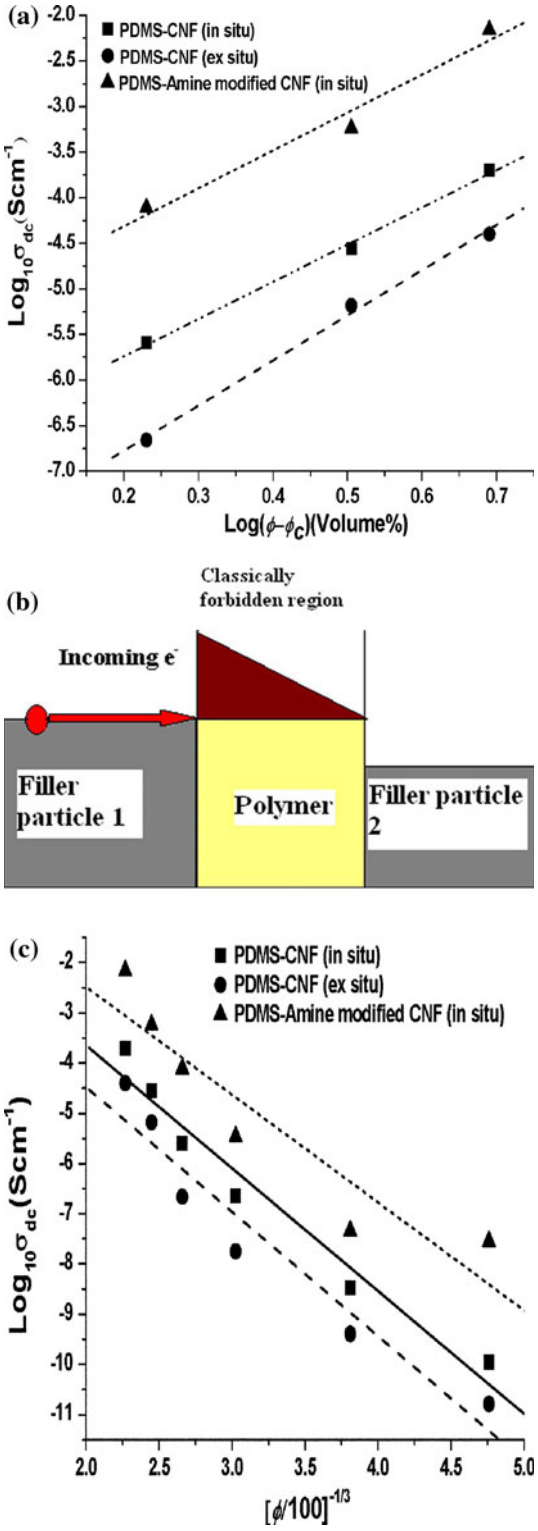

Fig. 7 **a** Plot of Log σ_{dc} versus Log $(\phi - \phi_c)$ for CNF-based nanocomposites. **b** Mechanism of tunneling conductivities in nanocomposites. **c** Logarithm of dc electrical conductivity versus $(\phi/100)^{-1/3}$

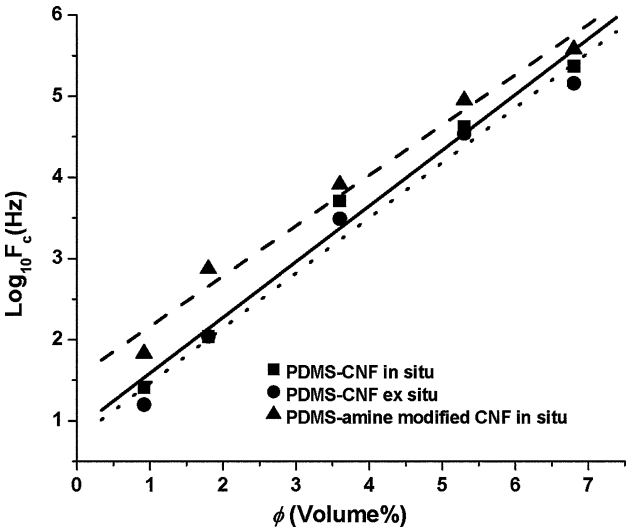

Fig. 8 Logarithm of critical frequency F_c as a function of filler volume percent

[34, 35]. The concept of the donor–acceptor interaction in this case arises from the structural similarity of the nanofibers with fullerenes. Fullerenes C_{60} are good electron acceptors, while amines are good electron donor and hence may form a charge transfer complex [33]. This may result in electron transfer from amines to nanofibers. The amine functionalized CNF aids proton transfer along the H-bond generated leading to a prominent increase in intrinsic conductivity. Thus, in this case disadvantage of functionalization is outweighed by improved dispersion of the nanofibers due to functionalization.

Effect of method of nanocomposite preparation and filler functionalization on dielectric constant

Dielectric constant ε', also known as permittivity, which is a measure of the energy stored in a cyclic electric excitation usually in the form of ionic charge layers depends on various factors. These are bulk permittivity, conductivity, size, shape, and spatial distribution of the filler in the matrix and the applied field frequency [36]. With increase in filler concentration, dielectric constant increases in magnitude. But for the polymer or the nanocomposites, it decreases with increase in applied frequency. Figure 9 depicts the change in dielectric constant with frequency at room temperature for unmodified and amine-modified CNF-based nanocomposites, respectively. For unmodified CNF-based nanocomposites, ε' decreases with increase in frequency, but the decrease is not prominent. However, for amine-modified CNF-based nanocomposites decrease in ε' is more prominent. Moreover, the magnitude of ε' increases with increase in filler loading. This increase is even more prominent for the amine-modified systems than unmodified

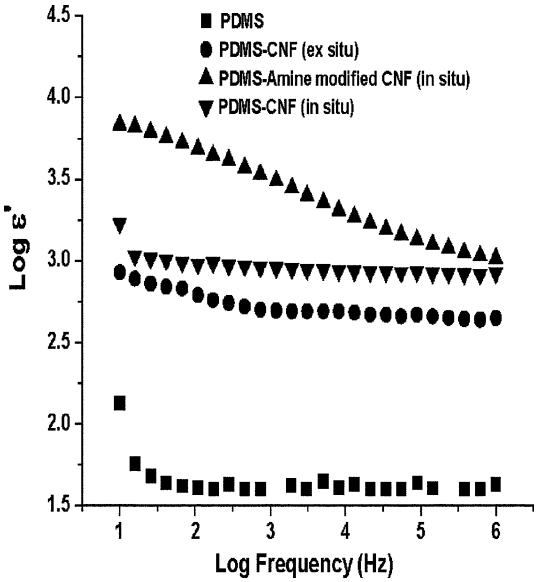

Fig. 9 Plot of Log ε' versus Log frequency for unfilled and CNF-filled PDMS nanocomposites

one. Unmodified (both in situ and ex situ) and amine-modified systems have reached percolation threshold at 4 and 1 phr of filler loading, respectively with marginal increase in ε' for higher filler loading. The reason behind these results is probably the difference in dispersion degree as is evident from TEM studies. Higher values of dielectric constant for amine-modified CNF-based nanocomposites is due to better filler dispersion compared with unmodified in situ and ex situ unmodified CNF-based nanocomposites with similar filler loading.

Conclusions

In situ preparation of CNF/hydroxyl PDMS nanocomposites was successfully carried out by anionic ring opening polymerization of octamethylcyclotetrasiloxane (D_4). Degree of dispersion was studied quantitatively by TEM analysis and by estimation of dispersion parameter $D_{0.1}$. In situ prepared nanocomposites were found to have a higher dispersion degree ($D_{0.1}$ of 24.56%) compared with conventional ex situ nanocomposites ($D_{0.1}$ of 11.26%). Moreover, functionalization of the CNFs gave a higher extent of dispersion ($D_{0.1}$ of 28.31%) as compared with unmodified CNF-based nanocomposites. Electrical properties were studied over a range of frequencies of the electric field. Percolation threshold was attained by amine functionalized CNF-based nanocomposites at a low filler volume fraction as compared with unmodified CNF based ones. This was because the filler conductive network was attained at much lower filler concentration. However, at the same filler loading for nanocomposites with unmodified CNF the conducting network formation was prevented due to filler agglomeration. For 1 phr loading of amine-modified CNF, dc conductivity (σ_{dc}) of the order of 10^{-8} Scm^{-1} was observed, while it had a magnitude of just 10^{-11} Scm^{-1} for ex situ prepared nanocomposites and 10^{-10} Scm^{-1} for in situ prepared nanocomposites with unmodified CNF. Below the critical threshold concentration, increased conductivity was due to tunnel conductivities in the nanocomposites which was evident from the linear nature of the plot for Log σ_{dc} versus $\sigma^{-1/3}$.

Acknowledgements The authors thank Council of Scientific and Industrial Research (CSIR), New Delhi for the financial grant supporting this study.

References

1. Whitesides GM (2005) Small 1:172
2. Luo JJ, Daniel IM (2003) Compos Sci Technol 63:1607
3. Logakis E, Pollatos E, Pandis Ch, Peoglos V, Zuburtikudis I, Delides CG, Vatalis A, Gjoka M, Syskakis E, Viras K, Pissis P (2010) Compos Sci Technol 70:328
4. Verdejo R, Werner P, Sandler J, Altstadt V, Shaffer MSP (2009) J Mater Sci 44:1427. doi:10.1007/s10853-008-3168-y
5. Stankovich S, Dikin DA, Dommett GHB, Kohlhaas KM, Zimney EJ, Stach EA, Piner RD, Nguyen ST, Ruoff RS (2006) Nature 442:282
6. Ahmad K, Pan W (2008) Compos Sci Technol 68:1321
7. Roy N, Bhowmick AK (2010) Polymer 51:5172
8. Ray SS, Okamoto M (2003) Prog Polym Sci 28:1539
9. Xu Y, Hoa SV (2008) Compos Sci Technol 68:854
10. Moniruzzaman M, Winey KI (2006) Macromolecules 39:5194
11. Guo H, Rasheed A, Minus ML, Kumar S (2008) J Mater Sci 43:4363. doi:10.1007/s10853-008-2556-7
12. Lin Y, Böker A, He J, Sill K, Xiang H, Abetz C, Li X, Wang J, Emrick T, Long S, Wang Q, Balazs A, Russell TP (2005) Nature 434:55
13. Balazs AC, Emrick T, Russell TP (2006) Science 314:1107
14. Owen MJ (1990) Siloxane surface activity, silicone-based polymer science: a comprehensive resource. American Chemical Society, Washington
15. Finegan IC, Tibbetts GG, Glasgow DG, Ting J-M, Lake ML (2003) J Mater Sci 38:3485. doi:110.1023/A:1025109103511
16. George JJ, Bhowmick AK (2008) Nanoscale Res Lett 3:508
17. Luo ZP, Koo JH (2007) J Microsc 225:118
18. Luo ZP, Koo JH (2008) Polymer 49:1841
19. Luo ZP, Koo JH (2008) Mater Lett 62:3493
20. Linares A, Canalda JC, Cagiao ME, García-Gutiérrez MC, Nogales A, Martín-Gullón I, Vera J, Ezquerra TA (2008) Macromolecules 41:7090
21. Stauffer D (1985) Introduction to percolation theory. Taylor & Francis, London
22. Kirkpatrick S (1973) Rev Mod Phys 45:574
23. Kilbride BE, Coleman JN, Fraysse J, Fournet P, Cadek M, Drury A, Hutzler S, Roth S, Blau WJ (2002) J Appl Phys 92:4024
24. Barrau S, Demont P, Peigney A, Laurent C, Lacabanne C (2003) Macromolecules 36:5187
25. Sandler JKW, Kirk JE, Kinloch IA, Shaffer MSP, Windle AH (2003) Polymer 44:5893
26. Quivy A, Deltour R, Jansen AGM, Wyder P (1989) Phys Rev B 39:1026

27. Celzard A, McRae E, Marêché JF, Furdin G, Dufort M, Deleuze C (1996) J Phys Chem Solids 57:715
28. Sichel EK (ed) (1982) Carbon black polymer composites. Marcel Dekker, New York
29. Sichel EK, Gittleman JI, Sheng P (1978) Phys Rev B 18:5712
30. Ezquerra TA, Kulescza M, Balta′-Calleja FJ (1991) Synth Met 41:915
31. Connor MT, Roy S, Ezquerra TA, Balta′-Calleja FJ (1998) Phys Rev B 57:2286
32. Boettger H, Bryksin UV (1986) Hopping conduction in solids. Akademie Verlag, Berlin, p 108
33. Valentini L, Armentano I, Puglia D, Kenny JM (2004) Carbon 42:323
34. Hirsch A, Li QY, Wudl F (1991) Int Ed Engl 30:1309
35. Bokobza L (2007) Polymer 48:4907
36. George JJ, Bhadra S, Bhowmick AK (2010) Polym Compos 31:218